THE INTERMETALLIC PHASES OF TITANIUM-BERYLLIUM

by

JOHN EDWARD LAWRENCE

B. A., Occidental College, 1959

A THESIS

submitted in partial fulfillment of the

requirements for the degree

MASTER OF SCIENCE

Department of Physics

KANSAS STATE UNIVERSITY
Manhattan, Kansas

1961

TABLE OF CONTENTS

LIST OF PLATES AND TABLES

INTRODUCTION

Various factors govern the alloying of metals that frequently create structures characterized by neither parent material. The terms intermetallic phase and intermediate phase are most commonly used to describe such alloying structures.

The importance of the connection between the physical properties and constitution is widely recognized. For if it were possible to predict with certainty what kind of constitution would be obtained by adding certain substances to a given solvent metal, the way would lie open for the production of alloys with predetermined properties. Therefore the knowledge of a constitution diagram is a prerequisite for predicting a composition with unique properties.

Many factors must be considered when stabilizing a given metallic structure. The influence of the ratio of valency electrons to atoms is a factor often found useful. Linus Pauling (6) has indicated that covalent bonding forms the basis for this ratio. The relative size of the atom in an aggregate of different types of atoms was a factor put forward by Laves. A consideration of the ionic or electrochemical interactions has recently been applied to new intermetallic phases. There exist other factors besides the three just mentioned that are frequently found to be applicable to a particular intermetallic phase. However, those factors that apply for one phase may or may not apply strikingly for another. The consideration put forward by Laves was found extremely useful in the study of the binary system of

titanium-beryllium.

Laves phases refer to an important group of intermetallic phases consisting of elements whose atomic diameters d_A and d_B are approximately in the ratio 1.2:1. This type of intermetallic phase has been observed for ratios from 1.1 to 1.6:1. Three structural types of approximate formula AB_2, compose the Laves phases.

1. The C_{14} structure, typified by the phase $MgZn_2$, hexagonal, with packing ABABAB.
2. The C_{15} structure, typified by the phase $MgCu_2$, cubic, with packing ABCABCABC.
3. The C_{36} structure, typified by the phase $MgNi_2$, hexagonal, with packing ABACABAC.

The chief reason for the existence of these phases is very likely to be purely geometrical. Witte and co-workers (3) have experimentally confirmed the existence of a strong magnetic susceptibility in Pseudo-Binary sections of $MgCu_2$-$MgZn_2$ and $MgNi_2$-$MgZn_2$.

The previously mentioned factors were applied to the binary system of titanium-beryllium as early as 1936. Misch (4) at that time reported the existence of a Be_2Ti phase. This was the first announcement of an intermetallic phase in the titanium-beryllium system. Later in 1949, P. Ehrlich (1) published his observation on eleven compositions from pure titanium to pure beryllium. These were made from x-ray powder photographs using CuK_α-radiation. In this paper he reported the existence of a BeTi phase, Be_2Ti phase, and a Be_4Ti phase. Ehrlich supported Misch's

description of Be_2Ti as face-centered cubic, C_{15} type, structure. Even though Ehrlich had reported the existence of the BeTi and Be_4Ti phases, he did not determine their structures. The last of the early publications that announced the existence of new single phases within this binary system was by Raeuchle and Rundle (7). Their description of $Be_{12}Ti$ as a disordered hexagonal structure was made possible from single crystal Weissenberg and precession photographs.

New information relative to the intermetallic phases of the titanium-beryllium system has appeared within the last eighteen months. Paine and Carrabine (5) used power diffraction patterns from CuK_α radiation to detect a $Be_{17}Ti_2$ phase which was isomorphous to Nb_2Be_{17}. This constitution was partially confirmed using x-ray powder methods, by Zalkin, Sands, Bedford, and Krikorian (10) who reported that $Be_{17}Ti_2$ exhibited two different structures. The α form associated with the Be-poor side of $Be_{17}Ti_2$ was isomorphous with the Nb_2Be_{17} type. The β form was reported to be isomorphous with the Th_2Ni_{17} type and associated with the Be-rich side. Be_3Ti was also found and reported by this group to be hexagonal.

Several intermetallic phases of the titanium-beryllium system have been reported. The five mentioned references announce the existence of structures that in several instances are not wholly agreed upon. As an example, Ehrlich reports that Be_3Ti consists of two phases, Be_2Ti and Be_4Ti. Zalkin, Sands, Bedford, and Krikorian describe Be_3Ti as a single phase region with a hexagonal structure. A particular single phase cannot be

definitely established until its structure has been determined. Therefore BeTi and Be_4Ti must be investigated to establish their existence. Paine and Carrabine did not report the β-$Be_{17}Ti_2$ phase that was later announced. Zalkin, Sands, Bedford, and Krikorian stated that the disordered hexagonal $TiBe_{12}$ reported by Raeuchle and Rundle (1952) was not observed in their powder patterns. Laves suggested that the conditions that satisfy the C_{15} type structure also satisfy the C_{14} and C_{36} type structures. Could the C_{14} or the C_{36} type structures be present in Be_2Ti since Misch and Ehrlich agree that it is isomorphous with the Laves C_{15} type structure?

The purpose of this report is to supply continuity to the existing intermetallic phases and to detect and explain new structures if disagreement is found. Witte (3) has detected unique magnetic susceptibility properties in the Laves phases. The cubic Be_2Ti is the only intermetallic phase that has been agreed upon by two references. Assuming Be_2Ti possesses unique susceptibility properties, the region through which this phase exists as well as how the parameters change within this region are vital to an interpretation of the magnetic susceptibility as well as its other properties. Therefore, since information has been gained for compositions at room temperature, a room temperature analysis of an equilibrium established at high temperature over the same range of composition is needed. One purpose of this report is to supply this needed information. The confusion associated with $Be_{17}Ti_2$ and $Be_{12}Ti$ could be reduced if high temperature structural data are found to support one of the conflicting

references. At the present time, all the reports relative to this binary system have either neglected to define the temperature state of investigation or have stated it as room temperature.

In order to obtain high temperature structural data, specimens of various compositions over the range of interest were heated to a high temperature and permitted to remain at that temperature until the equilibrium phase had been established within the specimen. The specimens were then cooled quickly to maintain the structure characteristic of that high temperature. X-ray diffraction powder techniques were used to analyze the quenched specimens. These samples were also analyzed metallographically in order to gain a more thorough understanding of the multiphase regions. To avoid the long and tedious mathematics involved in structural determination, the IBM-650 magnetic drum computer was employed for the longer routine calculations.

APPARATUS AND PROCEDURE

Specimen Characteristics

Beryllium (9) has been widely used in industry for many years. Presently it is being used as a moderating material for nuclear reactors.

The inhalation of beryllium or beryllium compounds as vapor, dust, or mist into the body can cause either an acute or a delayed chemical pneumonitis. Ulceration and irritation of the skin have been observed and are thought to be caused by beryllium or

beryllium compounds getting into breaks in the skin. However, the most serious pathology is within the lungs. The more recent information seems to indicate that beryllium in any form can be toxic. There is no specific treatment.

Titanium (9) has been used by scientists and engineers as a light weight strength inducing material. This metal has shown unusual corrosion resistance to salt water.

There are no reported cases in literature where titanium as such has caused any toxic effects.

Beryllium reacts readily with oxygen to form BeO. It has also been found to react readily with silica to form beryllium orthosilicate Be_2SiO_4.

Titanium readily reacts with oxygen to form TiO, TiO_2, as well as Ti_2O_3 and Ti_3O_5. This substance will also react with silicon in the absence of oxygen to form Ti_5Si_3, TiSi, and $TiSi_2$.

The precautions taken on this project to avoid the toxic properties of beryllium and the contamination of the specimens will be emphasized in this report.

Preparation of Alloys

Eight compositions were selected that were characteristic of the three regions reported in literature. Three of the eight specimens were prepared to yield structural data about the reported Be_2Ti phase. These were a Be_3Ti_2, Be_5Ti_2, and Be_3Ti. Be_4Ti was also prepared to check Ehrlich's prediction. In order to clarify the conflicting reports of the $Be_{17}Ti_2$ phase, three

specimens were prepared: Be_5Ti, Be_6Ti, and Be_7Ti. The last of the three regions of investigations was associated with $Be_{12}Ti$. A specimen of $Be_{12}Ti$ was prepared for this purpose.

Beryllium was obtained in powder form as 98-99 per cent Be with silicon as an impurity. Titanium was obtained in sponge form. After the desired compositions were prepared, they were pressed into cylindrical forms approximately two inches in diameter and one-half inch thick. Solid ingots were made from these forms by an arc melting technique within an inert atmosphere. This method was employed since it avoided the possibility of contamination characteristic in many furnace melting methods. The employed method was not entirely satisfactory, for during the arcing process beryllium was lost creating beryllium-poor samples of several compositions.

The resulting chemical compositions were checked by the Union Carbide Metals Company and found to be as shown in Table 1.

Table 1.

Specimen one	22.80 ± 0.10% Be
Specimen two	30.00 ± 0.19% Be
Specimen three	33.17 ± 0.22% Be
Specimen four	46.40 ± 0.18% Be
Specimen five	44.01 ± 0.15% Be
Specimen six	51.29 ± 0.16% Be
Specimen seven	51.87 ± 0.13% Be
Specimen eight	68.81 ± 0.27% Be

Small pieces, approximately one-quarter inch on a side, were taken from each of the eight ingots. These samples were then prepared for the heat treatment by first placing each specimen

in a well marked pure titanium capsule. This was to shield the readily reacting silica glass from the specimens. In order to avoid further contamination of the samples at high temperatures the capsules were sealed in a quartz tube under partial pressure of argon. Plate I, Fig. 2, illustrates the sealing apparatus. The quartz tube was flushed four times with argon and evacuated after each flushing.

Contamination to the eight samples would most likely be due to the titanium within the specimens reacting with the silica of the tube, since this was an oxygen free region. Beryllium was isolated since it could neither react with oxygen nor with the silica in the oxygen free chamber. Titanium from the capsule could react with the beryllium within the specimen, but this was unlikely at the heat treating temperature. Whenever possible the titanium-beryllium specimens were handled in a "dry box" or with tweezers and gloves in a well ventilated room. All instruments as well as the immediate area were washed thoroughly each time after the samples were handled.

Furnace

In order to obtain a room temperature analysis of an equilibrium established at a high temperature, the tubes containing the specimens were first heated in an electric furnace. The melting points of beryllium and titanium are 1283° C and 1800° C, respectively. For this intermetallic phase study a temperature

near 1000° C was selected. By choosing this temperature the phases containing liquid beryllium were believed to be avoided, yet diffusion of the metal atoms would take place during the heat treatment.

The basic requirements for this furnace were as follows. The furnace must be able to withstand a temperature of 1050° C for a long period of time. The fluctuation in temperature must not be greater than ±15° C and preferably ±5° C. The region of uniform temperature must be large enough to hold eight four-inch tubes.

A Hoskins Electric Furnace type FD204C met the above specifications after minor alterations were made on the chamber and sliding door. A brick riser was placed in the furnace to enable the specimens to be at the center of the chamber where the temperature was being determined. A transite plug with holes for chromel-alumel thermocouple wires was placed in a viewing port of the door. This thermocouple was used to calibrate the heat-regulating device.

The heat-regulating circuit is shown in Plate I, Fig. 1. The illustrated circuit contains a bimetallic strip that controls a microswitch. When the bimetallic material is cool the microswitch remains in a closed position, permitting the coils to carry current. However, when the bimetallic strip becomes hot, it will break the microswitch and thus stop the current in the heating coils. When the coil circuit is closed, approximately 20 amperes of current pass to heat the furnace. The bimetallic material will heat whenever the microswitch is closed.

EXPLANATION OF PLATE I

Fig. 1. Temperature regulating circuit (Hoskins Electric Furnace Type FD204C).

1. Single pole double throw switch.
2. Bimetallic strip heater.
3. Microswitch.
4. Relay coils.
5. Rheostat.
6. Switch.
7. Relay contacts.
8. 15-ampere fuses.
9. Light.

Fig. 2. Specimen encapsulation apparatus.

1. To argon source.
2. To vacuum.
3. Triple port stopcock.
4. Flexible tubing.
5. Quartz tubing.
6. Region to be sealed.
7. Titanium capsule.
8. Titanium-beryllium specimen.

PLATE I

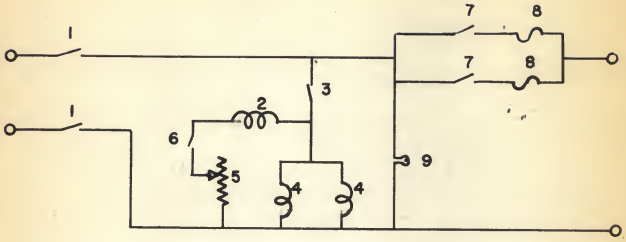

Fig. 1.

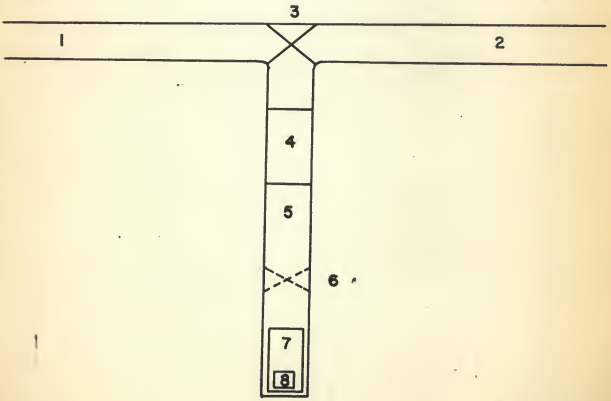

Fig. 2.

The current through the bimetallic strip can be regulated by a rheostat or stopped completely. By adjusting the rheostat the heating period of the furnace can be governed.

A voltage regulator was not available, thus requiring the furnace to be calibrated for a period of one week. The line current was found to be more stable during a period from Friday to Monday than for any other equal period. Chromel-alumel thermocouples and a potentiometer were used for calibration as well as to determine the heating rate and heating period. During this calibrating process and the heat treatment, readings were taken every four hours to detect any major temperature fluctuations.

Heat Treatment and Quenching

The constitution and structure of the specimens depends not only on their composition but also on the thermal and mechanical treatment to which they have been subjected. However, the thermal and mechanical history of the specimens can be erased if the samples are subjected to a high temperature for a long period of time. The period for which an alloy should be heat treated depends on several factors. One factor considers the ability of an atom to move within the lattice at any given temperature. An unreasonable length of heat treatment time is necessary for some materials to acquire an equilibrium structure at a given temperature. This may occur if the atoms within the material are not given sufficient energy to overcome the energy barrier for diffusion to an equilibrium state. The probability of obtaining this

state is proportional to $e^{-U/KT}$, where U is the barrier energy, K is Boltzmann's constant, and T is the temperature in degrees Kelvin.

The eight specimens were heat treated at 1026 ±25° C for a period of 67 hours 20 minutes. The atomic weight of beryllium and titanium is 9.013 and 47.90 grams per mole, respectively. Beryllium has only four electrons and is 75 per cent the diameter of the titanium atom. Therefore the beryllium atoms should move freely within the lattice at the heat treatment temperature.

Rapid quenching was used in order to retain for examination at room temperature the constitution corresponding to the state of the specimens during the high temperature treatment. In general, there are some processes of transformation in metals and alloys which cannot be suppressed entirely, or even partially, by the most rapid quenching even to very low temperatures.

The eight specimens used in this structural analysis were quenched in air to a room temperature of 33° C. The quenching time from 1026° C to 33° C required from three to four minutes.

The quenching rate was restricted due to the quartz tube enclosing the sample. Quartz was used because of its ability to retain its form at 1000° C. However, it was found to break if placed in water while still "orange" hot. This could not be permitted due to the possibility of oxides and hydrides contaminating the specimens.

Preparation Precautions

The powder method of x-ray analysis is most generally used in the study of intermetallic phases and was applied to this investigation. This technique brings with it certain special precautions that are nonexistent in other methods, such as those using single crystals. If these precautions are not met, the samples may become contaminated, strained, or lose their identity as associated with a particular heat treated composition.

In order to avoid the mixing of samples, only one specimen was handled at a time. This includes the time from opening the quartz tube to placing the x-ray powder sample into its own well marked container. The mixing of samples at this point could possibly lead to an uncalculated misjudgment.

The quartz tube was broken to remove the titanium capsule containing the specimens. The small pieces of the heat treated material were then removed from the titanium capsule and placed in a small agate mortar. The larger pieces were then placed in a well marked container to later be used in a metallographic examination.

Special precautions were taken while grinding the remaining pieces of the specimen. As an example, to avoid the possibility of contamination, any small piece that fell from the mortar was not replaced. All pieces in the mortar were ground thoroughly with full consideration that in a two-phase region, one phase will resist grinding more than the other.

The finely ground powders were placed on an extremely clean

piece of paper. Duco cement was mixed with the powder and the mixture was rolled into thin rods approximately one millimeter in diameter. Each needle was mounted on the tip of a glass rod to prevent the contamination of the powder camera.

Every container holding a specimen was filled and sealed in argon to prevent the formation of oxides.

The greatest precaution taken throughout the specimen preparation was the containment of the dangerous powders, dust, and vapors associated with the material. Whenever the samples were handled, whether as part of the ingot, as small pieces, or as powder needles, the same protective plastic sheet was worked on to catch the waste. This sheet was cleaned thoroughly and saved after each use.

X-ray Studies

X-ray diffraction provides the only consistent means of determining the crystal structures on an intermetallic compound. If a single crystal is available, diffraction techniques may be employed to analyze its structure quite accurately. However, single crystals are seldom available when the intermetallic phase analysis is desired. The method most frequently applied to polycrystalline materials is the powder diffraction technique.

This method requires a near monochromatic beam to fall incident upon the powder sample. The diffracted beams that leave the sample define cones of radiation whose axis lies along the direction of the incident beam. Each cone of rays is diffracted from

a particular set of lattice planes. A narrow strip of film is used to record the positions of the cones of radiation. A Straumanis type powder camera, 57.3 mm in diameter, was used in this investigation. Bragg's law provides a means of relating each diffraction cone to a set of lattice planes.

The monochromatic beam employed in the powder diffraction methods refers to the strong Kα component of the characteristic radiation from the x-ray tube. Copper radiation was used for its atomic number is further away from the specimens constituents' atomic numbers, thus restricting the fluorescent radiation caused by the incident radiation having a wavelength near the K-edge of the target material. Molybdenum has a greater atomic number than copper. However, this small wavelength is accompanied by poor resolution.

A nickel filter was used to reduce the CuKβ radiation to a near background intensity. The true absorption factor presented an early problem in this investigation. This factor is caused by electronic transitions within the atom.

A photon of sufficient energy can remove a K-electron from an atom. The electron which falls from an outer shell to fill the vacancy created by the absent K-electron may produce radiation. The emitted radiation is called fluorescent radiation and is characteristic of the target or sample initially irradiated. The fluorescent radiation in this problem was from titanium at a wavelength λ = 2.497 A, while the coherently scattered CuKα radiation has a wavelength λ = 1.542 A. A large amount of this fluorescent radiation was producing a background that masked all

but a few diffraction lines. An aluminum sheet of 2.3-mil thickness was cut to the same dimensions as the film and placed between the film and the powder needle to absorb the fluorescence. The aluminum absorbs the longer wavelength from titanium, but does not appreciably absorb the higher energy copper radiation.

Metallography

A well established method for the investigation of the structure and constitution of metals and alloys is that of metallographic examination. Small chunks of each of the eight specimens were mounted individually in Lucite prior to their polishing and etching. The mounting was accomplished by placing Lucite powder and a piece of the heat treated specimen in a hydraulic press. The Lucite powder transformed into a clear solid form when heated to 135° C and pressed with 4000 psi pressure for 20 minutes. In the solid form the Lucite cylinder was one and one-fourth inches in diameter and approximately three-fourths inch thick with the specimen near a plane surface.

The polishing was accomplished in three steps. The first involved an extremely coarse grinding paper. This 100-gauge paper was used to remove the thin layer of Lucite covering the specimen as well as a thin layer of sample in order to expose a large cross section of the material. Then a 50-gauge paper replaced the previous paper. This grinding paper was used to remove the scratches created by the 100-gauge paper and to reach a typical cross section of the particular sample. All of the

grinding during this first step was done in a "dry box" to restrict the dangerous effects of the beryllium within the grinding waste and air.

The second step in the preparation of a polished surface was accomplished by using emery paper of increasingly finer grades. First a 40-micron paper was used, followed by a 20-micron paper. The samples were checked several times during the grinding. A finer grade of paper was used when the scratches of the previous paper were replaced by the scratches of the paper then being used.

The last of the three steps leading to a finely polished surface required a polishing cloth impregnated with fine abrasive powders. These powders range from 40 microns to one-half micron. The first powder used for our samples was of the 20-micron grade. This was followed by the 13-, 6-, and 1-micron grades. A polishing wheel was used during steps two and three for it enables the specimens to be polished more uniformly and rapidly. Tap water was used for the third step until the discovery that its impurities were making 40-micron scratches on the finely polished surfaces. Distilled water was used continuously after the tap water was discarded. The grinding wheel was cleaned thoroughly and the polishing cloth replaced each time a new powder was used. Gloves were used to avoid the harmful effects of the specimens.

When a polished surface, free from scratches, had been prepared, the quasi-amorphous surface layer was removed by etching. For the titanium-beryllium specimen eight per cent nitric acid and three per cent hydrofluoric were used as an etch. The

specimens and their Lucite molds were placed in this etch at room temperature for two minutes, then rinsed in alcohol. The formation of oxides on the highly polished and etched surfaces was prevented by the specimens being placed in a desiccator filled with argon.

The eight specimens were now ready to be investigated by an optical microscope. A study can now be made of the microstructures, grain structures, phases, and directional properties in the crystalline structures.

RESULTS

Methods

Several methods of analysis are available to the researcher interested in the intermetallic phases associated with a particular alloying system. Four methods generally used maintain little resemblance to one another, yet contribute greatly to a thorough understanding of an alloying system. The contribution of any one of these four methods would not enable a researcher to establish any more than a good theory or prediction of an intermediate phase's structure and constitution. In general, the various experimental techniques differ in sensitivity, and therefore in usefulness from one portion of the constitution diagram to another.

Thermal analysis is the best method for determining the liquidus and solidus, including eutectic and peritectic horizontals,

but it may fail to reveal the existence of eutectoid and peritectoid horizontals because of the sluggishness of some solid-state reaction or the small heat effects involved. The eutectoid and peritectoid horizontals are best determined by metallographic examination or x-ray diffraction, and the same applies to the determination of solvus curves. Due to these considerations the thermal method of analysis was not used in this investigation.

The metallographic approach may yield information about an intermetallic phase that could not be confirmed by any other means. This includes the relative types and positions of second or even third phases within an alloying system. This is also a powerful technique for determining the relative amounts of these phases. This well established and versatile approach lacks only one serious quality; that is the ability to determine the atomic arrangement within certain phases.

The use of the x-ray diffraction method provides a means of determining crystal symmetries, lattice parameters, as well as atomic positions within a unit lattice. This approach provides the final and most thorough method of intermetallic phase analysis.

The method of chemical analysis provides the researcher with a rule of composition that cannot be violated. If the phases in a multiphase region have been determined, then the relative amounts of these phases within a particular composition may be determined quite accurately by a chemical consideration. This method may also predict the existence of small amounts of a phase that may be overlooked by the x-ray and metallographic methods.

No one of the aforementioned methods can by itself provide the information for a complete understanding of an alloying system. Each method can provide information not detectable by the others. Yet there is also a fortunate overlap within the four methods that permits the checking of conclusions.

X-ray Analysis

Three regions of composition were prepared for this high temperature intermetallic phase analysis. The first region of compositions was composed of three specimens near Be_2Ti. Specimen one was on the titanium rich side of Be_2Ti, while specimen two was on the beryllium rich side of Be_2Ti, and specimen three was on the titanium rich side of Be_3Ti.

The Straumanis type powder films indicated at first glance that specimens one, two, and three were all characteristic of the same intermetallic phase. Each of the three films had enough of the same predominant diffraction lines to make this prediction. In order to analyze this region of constitution, calculations of d, the distance between atomic planes, and $1/d^2$ were made from the powder patterns. This confirmed the existence of a single region of constitution.

Approximately 29 lines could be read on these patterns, thus indicating the possibility of a structure of poor symmetry, a structure of high symmetry and an extremely large unit cell, or the existence of more than one phase. The first indication of a two-phase region came from a calculation of the difference in

$1/d^2$'s and the sum of the square of the Miller indices. Most of the dominant lines had the sum of the square of the Miller indices indicating a face-centered cubic phase. Assuming these lines were cubic, the lattice parameter was calculated for each dominant line and plotted against the square of the cosine of the angle corresponding to that particular diffraction line. By this means, one phase was isolated and found to be cubic with a lattice parameter of 6.460 ± 0.006A (Table 4).

The remaining lines were found to belong to a hexagonal structure of the C_{14} type by the use of a Hull-Davey chart. The parameters of this phase were determined to be a = 4.485 ± 0.005A and c = 7.161 ± 0.008A (Table 5).

The structures were established when the intensity check using the atom positions of the Laves C_{14} and C_{15} type structures agreed with the observed intensities.

The relative amounts of the two phases were determined for each composition by observing the relative intensities of the two phases comprising the constitution. Specimen one (Table 7) is predicted to be 80 per cent cubic, while specimen two (Table 8) is approximately 80 per cent cubic, and specimen three (Table 9) is about 70 per cent cubic.

The second region of constitution to be investigated consisted of specimens with compositions between Be_4Ti and Be_6Ti. Specimens four and five were on the beryllium rich side of Be_4Ti, while specimens six and seven were on the titanium rich side of Be_6Ti. The powder patterns of these four specimens possessed a

great resemblance to one another. Each pattern had approximately 48 of the same diffraction lines. The patterns of specimens four and five were nearly identical in the number and values of d-spacings and the intensities of these lines. This comparison was found to apply to the pattern of specimens six and seven. However, even though the position of lines was nearly consistent within the four specimens' patterns, the intensity did change between the first pair of patterns and the last pair.

The absence of speckled lines and the very few dominant lines prevented the separation of the individual phases by this means. The diffraction lines of the hexagonal phase found in the patterns from the first three samples were absent. However, lines were found of weak intensity that could be attributed to the cubic phase found in specimens one, two, and three. The removal of these lines from consideration left approximately 30 lines. A check of the Hull-Davey chart indicated that most of them could belong to a hexagonal structure whose parameters were similar to those reported in literature as α-$Be_{17}Ti_2$. These parameters were found to be a = 7.454 ± 0.003A and c = 10.72 ± 0.07A (Table 6). A combination of these two structures accounted for the lines on the powder patterns of specimen four and specimen five. A close examination disclosed the existence of lines on the patterns of specimens six and seven that could not be explained by cubic and hexagonal structures of the two previous specimens. These lines were found to correspond to the dominant lines found on the pattern of specimen eight. Specimens six and seven were therefore found by x-ray diffraction

techniques to consist of three phases: the cubic phase found in the first three specimens, the hexagonal phase found in specimens four and five, and small amounts of a new phase observed in specimen eight.

An intensity check using the cubic atomic positions of the C_{15} type structure and the hexagonal atomic positions reported for Nb_2Be_{17} proved the existence of the two phases in specimens four through seven.

The relative amounts of these two phases within the four specimens could only be vaguely predicted. Specimen four (Table 10) is approximately 50 per cent cubic and 50 per cent hexagonal. Specimen five (Table 11) is near 60 per cent cubic, and 40 per cent hexagonal. Specimen six (Table 12) is approximately 40 per cent cubic, 50 per cent hexagonal, and 10 per cent of the specimen eight's dominant phase. Specimen seven (Table 13) is 35 per cent cubic, 50 per cent hexagonal, and 15 per cent of the specimen eight's dominant structure.

Specimen eight is similar to $Be_{12}Ti$ in composition. Even though this specimen's diffraction pattern had 37 lines, a dominant cubic phase could easily be separated from the other. The lattice parameter of this cubic phase was found to be a = 7.38 ± 0.02A (Table 14). The second phase consisting of low intensity lines was found to be due to a hexagonal phase with the Nb_2Be_{17} type structure. Approximately 90 per cent of this region consists of the cubic phase with the remaining 10 per cent hexagonal.

A second heat treatment under identical thermal conditions using samples from the corresponding ingots as the first heat

treatment produced the same phases as the first treatment. However, more of the C_{14} type structure appeared on the first three specimens' photographs. More of the hexagonal Nb_2Be_{17} type structure was found in viewing the other specimens' films that were part of the second heat treatment than found in reading the previous corresponding films. Diffraction lines of the β-$Be_{17}Ti_2$ phase could be separate from the cubic phase on the film of specimen eight's second heat-treated sample.

Specimen two of the first heat treatment was found by x-ray means to be greatly contaminated by pure titanium. The x-ray films used to analyze specimen two were therefore of the second heat treatment. All other intermetallic phase analyses were made from the first heat-treated specimens. Titanium silicide lines were observed on the diffraction films of the first three specimens.

Metallographic Analysis

One limitation of the metallographic method of analysis is that all results are deduced from a small cross section of the specimen. The importance of obtaining a typical cross section cannot be minimized. One method used to separate the phases of a multiphase region is to rotate the specimen in polarized light and observe the relative changes in the reflected intensity from each phase by a high powered microscope. The Leitz Ortholux microscope "ultrapak" attachment was used for this purpose.

The metallographic pictures on plates two and three yielded a considerable amount of information about the types and amounts of phases within the eight specimens.

Specimen one was found to be three phased under polarized light. The dominant phase was optically isotropic and comprised approximately 80 per cent of the cross section investigated. The remaining 18 per cent was optically anisotropic. A magnification of 225 times made the separation of phases quite clear. The anisotropic phase appeared as long slender striations, some as wide as 0.05 mm. A third phase of approximately 1 or 2 per cent had no common geometric characteristics.

The metallographic examination was applied to the eight samples that were heat treated first. The second specimen did not possess the degree of homogeneity found in the other eight specimens investigated. Very little resemblance could be found in a comparison of samples one and two. One section of the second specimen appeared to be three phased with one phase approximately 20 per cent isotropic. Another section appeared to be composed entirely of an anisotropic phase. The overall specimen appeared to be 40 per cent strongly anisotropic and 60 per cent moderately anisotropic.

The third specimen appeared, as did specimen one, to be quite homogeneous. On first glance, there were no obvious similarities between specimens two and three. In contrast, specimens one and three bore many similarities. The general background that comprised 90 per cent of the section investigated was found to be weakly anisotropic under polarized light. However, this

may be isotropic and appear weakly anisotropic due to the specimen being strained. This surface appeared to have been more etched than the others. The remaining 10 per cent of the investigated cross section was strongly anisotropic and was grouped into long slender striations similar to those found in specimen one's minor phase. These striations were as wide as 0.04 mm.

Specimen four possessed neither the solid isotropic background nor the striations found in samples three and one. A new phase appeared that lacked order and consistency. This phase was weakly anisotropic and comprised approximately 30 per cent of the analyzed surface. On a metallographic picture this phase was quite light. Rows of this phase were separated by a dominant isotropic phase which accounted for 70 per cent of the surface.

The alternating rows of isotropic and anisotropic phases found in specimen four was also found in specimen five. The weakly anisotropic rows were quite well defined and comprised 50 per cent of the two phased region of investigation. The remaining 50 per cent was isotropic and gave slight indications of excess etching.

Specimen six did not possess well defined phases. A slight resemblance was found between the anisotropic phase of specimen four and the more dominant anisotropic phase which comprised 70 per cent of the investigated cross section of specimen six. The isotropic phase which consisted of the remaining 30 per cent of the cross section appeared blue. This isotropic phase was not grouped in a large section, but scattered throughout the

EXPLANATION OF PLATE II

Metallographic pictures of specimens, magnification 225 times.

Fig. 1. Specimen one.

Dark region	80% isotropic.
Gray region	18% anisotropic.
Light region	2% strongly anisotropic.

Fig. 2. Specimen two.

This specimen resulted from the first heat treatment and indicates strong contamination.

Fig. 3. Specimen three.

Gray region	90% weakly anisotropic.
Light region	10% strongly anisotropic.

Fig. 4. Specimen four.

Gray region	70% isotropic (blue).
Light region	30% anisotropic.

PLATE II

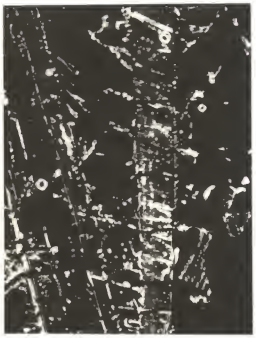

Fig. 1.

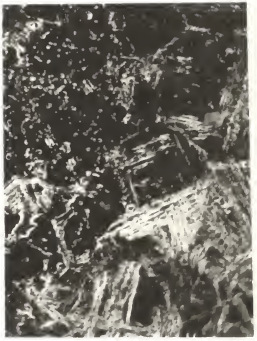

Fig. 2.

Fig. 3.

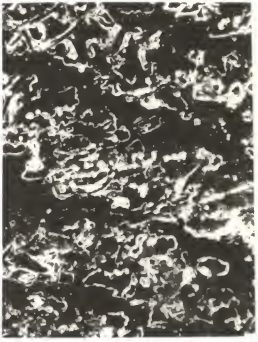

Fig. 4.

EXPLANATION OF PLATE III

Metallographic pictures of specimens, magnification 225 times.

Fig. 1. Specimen five

Gray region	50% isotropic (blue).
Light region	50% anisotropic.

Fig. 2. Specimen six.

Dark region	20% isotropic.
Light region	70% anisotropic.
Black region	10% isotropic.

Fig. 3. Specimen seven.

Dark region	40% isotropic (blue).
Light region	60% anisotropic.

Fig. 4. Specimen eight.

Black region	90% isotropic.
Light region	10% anisotropic.

PLATE III

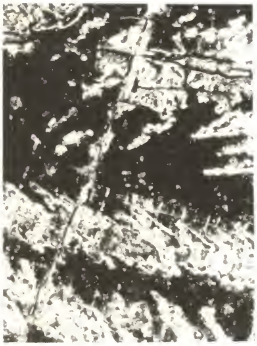

Fig. 1.

Fig. 2.

Fig. 3.

Fig. 4.

anisotropic phase.

The seventh specimen resembled the previous sample by having no consistent boundaries of a particular geometric shape. However, the boundaries that separated the isotropic phase from the anisotropic phase were generally well defined. The isotropic phase appeared blue and comprised 40 per cent of the surface. This phase appeared in many small but well defined groups. The anisotropic phase was quite similar to the dominant phase found in specimen six.

The last specimen bore little or no resemblance to any of the seven mentioned specimens. Under polarized light it appeared to be 90 per cent isotropic. The isotropic regions were shaped in long sections as wide as .15 mm. Each long section began or ended with a 60° angle at a point resembling a needle. An anisotropic phase of approximately 5 or 10 per cent separated the large isotropic regions.

Density

A theoretical density was calculated for each specimen prior to the formation of the ingots. Even though the compositions did change considerably during the arcing process, the theoretical values were still close enough to the true density to be used in determining the number of molecular units per unit cell of the different structures found by x-ray means.

The relative amounts of the determined phases comprising a particular specimen were ascertained using the theoretical

densities calculated for each specimen. Specimen one was found by this means to be 94 per cent C_{15} type cubic and 6 per cent C_{14} type hexagonal. Specimen two was found to be 39 per cent C_{15} type cubic and 61 per cent C_{14} type hexagonal. The third specimen was 24 per cent C_{15} type cubic and 76 per cent C_{14} type hexagonal. The difference between the apparent density and the theoretical density prevented the determination by this means of specimen four. Specimen five is 59 per cent C_{15} type cubic and 41 per cent of the Nb_2Be_{17} type hexagonal structure. Specimen six was found to consist of 46 per cent C_{15} type cubic, 44 per cent Nb_2Be_{17} type hexagonal, and 10 per cent $Be_{12}Ti$ cubic. Specimen seven was found to be 37 per cent cubic, C_{15} type structure, 53 per cent hexagonal α-Nb_2Be_{17}, and 10 per cent $Be_{12}Ti$ cubic. The eighth specimen was found to be primarily cubic with four molecular units per unit cell. However, the amount of a second phase could not be determined because of the large calculated density.

Chemical Composition

The phases found by the x-ray method were checked by a consideration of their chemical compositions. A prediction of the relative amounts of these phases could be determined for each specimen by this means.

Specimen one is comprised primarily of the C_{14} and C_{15} type structures, but must have small amounts of a titanium phase to balance the chemical equation. The second and third specimens

may also be comprised of the C_{14} and C_{15} type structures, but should also have small amounts of the beryllium rich Nb_2Be_{17} structure. However, the percentage of this is small and not detectable by x-ray diffraction methods. Specimens four and five should be two phased with a slightly dominant C_{14} or C_{15} type structure. The second phase should be 46 per cent of the Nb_2Be_{17} type structure. The sixth and seventh specimens could consist of a three-phase region which consisted of 26 per cent C_{15} type structure, 65 per cent Nb_2Be_{17} type structure and 9 per cent of the $Be_{12}Ti$ structure. If specimen eight consists of a cubic structure of the $Be_{12}Ti$ composition and a slight second phase, the amount of a second phase should be very small.

Computer

The existence of a particular structure in a material can initially be predicted by matching theoretical d-spacings with those observed experimentally. Final confirmation is obtained by comparing line for line the calculated intensities against the measured intensities. The atomic positions must be known in order to calculate a theoretical intensity. A calculation of the intensities is not difficult, but extremely tedious for a structure of low symmetry, large cell dimensions, or many atoms.

The IBM-650 data processing computer was programmed to compute the $1/d^2$ and structure factor squared values for all possible Miller indices within predetermined limits. The $1/d^2$ values allow the Miller indices and structure factor squared values to be

Table 2. Tabulation of the percentages of the phases present as found by the various methods.

	Cubic C_{15}	Hex C_{14}	Hex Nb_2Be_{17}	Cubic Spec 8	Unknown
Specimen 1					
X-ray	80	20			
Metallographic	80	18			2
Density	94	6			
Chemical	80	80			20 Ti
Specimen 2					
X-ray	80	20			
Density	39	61			
Chemical	91	91	9		
Specimen 3					
X-ray	70	30			
Metallographic	90	10			
Density	24	76			
Chemical	83	83	17		
Specimen 4					
X-ray	50		50		
Metallographic	70		30		
Chemical	54		46		
Specimen 5					
X-ray	60		40		
Metallographic	50		50		
Density	59		41		
Chemical	54		46		
Specimen 6					
X-ray	40		50	10	
Metallographic	30		70		
Density	46		44	10	
Chemical	26		65	9	

Table 2 (concl.).

	Cubic C_{15}	Hex C_{14}	Hex Nb_2Be_{17}	Cubic Spec 8	Unknown	
Specimen 7						
X-ray	35		50	15		
Metallographic	30		70			
Density	37		53	10		
Chemical	26		65	9		
Specimen 8						
X-ray				90	10	$Be_{17}Ti_2$
Metallographic				90	10	

compared with a particular observed diffraction line.

The input to the IBM-650 consisted of three sets of data. The first set is necessary to calculate the $1/d^2$ values. The general expression for $1/d^2$ may be written in the form

$$\frac{1}{d^2} = \epsilon_1 h^2 + \epsilon_2 k^2 + \epsilon_3 \ell^2 + \epsilon_4 hk + \epsilon_5 h\ell + \epsilon_6 k\ell$$

The values of the epsilons depend on the geometry and size of the unit cell. These values are put into the machine in the form of a non-load card. The last two words on this non-load card determine the maximum value of h and k (seventh word) and the maximum ℓ (eighth word).

The atomic scattering factors' polynomial coefficients (2) are placed on one-word-per-card load cards. The factor may be expressed in the form

$$f = a_0 + a_1 x + a_2 x^2 + a_3 x^3 + a_4 x^4 + a_5 x^5 + a_6 x^6$$

The x corresponds to 1/4d or $\sin\theta/2\lambda$ and is calculated using the epsilons placed in the machine. The locations of the coefficients

for beryllium are as follows: a_0-0883, a_1-0833, a_2-0783, a_3-0733, a_4-0683, a_5-0295, a_6-0792. The locations of the coefficients for titanium are as follows: a_0-0633, a_1-0583, a_2-0533, a_3-0483, a_4-0433, a_5-0742, a_6-0286.

The atomic positions are placed in the machine by putting each coordinate on a one-word-per-card load card. The first beryllium atom, for example, may be located at 1/2, 1/3, 1/4; so place 5000000050 in location 1701, 3333333350 in location 1801, and 2500000050 in 1901. The second beryllium atom's coordinates are placed in locations 1702, 1802, and 1902. The titanium atom's coordinates are placed in a similar manner in the 1400's, 1500's, and 1600's.

The output consists of h, k, l, $1/d^2$, F real, F imaginary, and F^2, in that order on a single card for each set of Miller indices. The general purpose board is used and the console is set to 7019510000+. The schematic diagram of this program which follows defines the major blocks of logic.

SCHEMATIC DIAGRAM

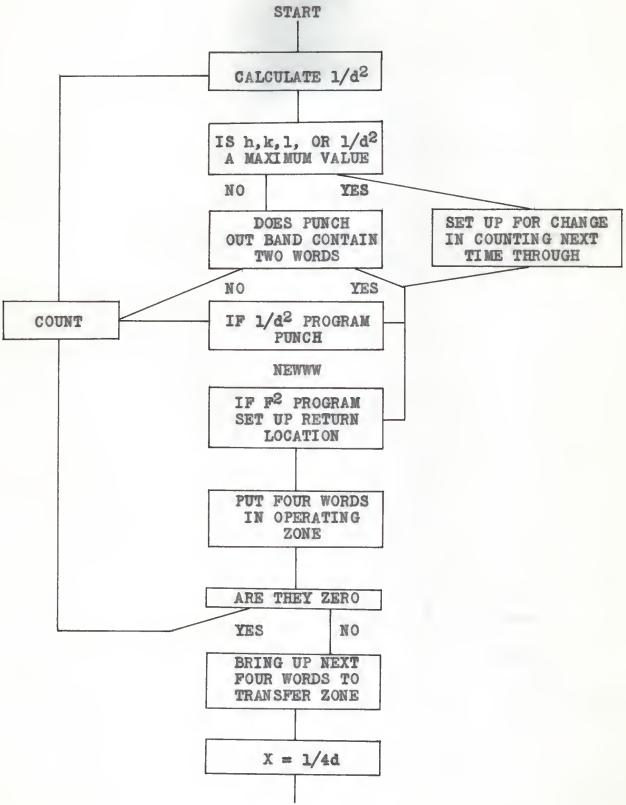

Schematic diagram (cont.).

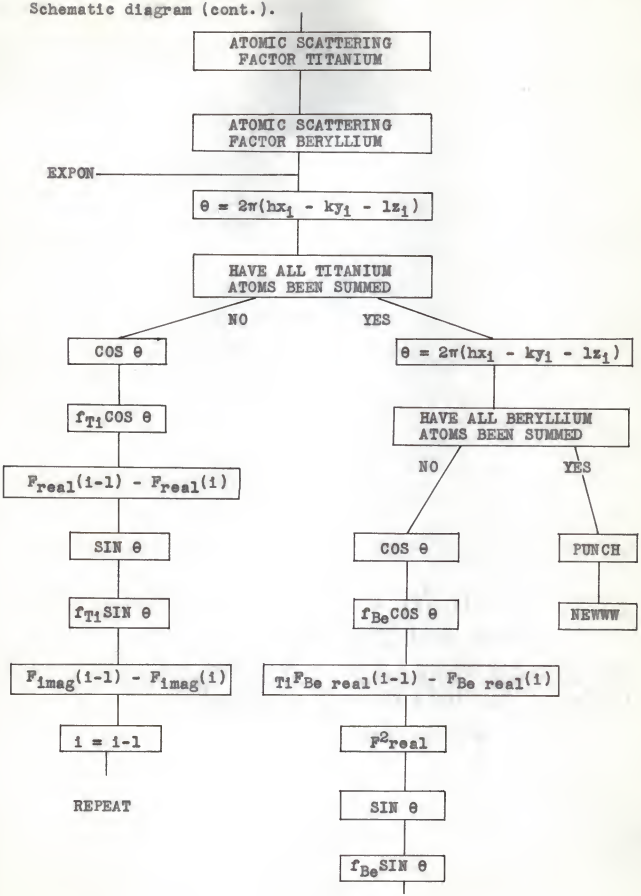

Schematic diagram (concl.).

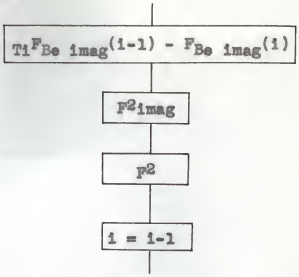

DISCUSSION

An investigation of the literature pertinent to the intermetallic phase analysis of the binary system of titanium-beryllium uncovered five reports. All were articles stating the discovery of single-phase regions of constitution from x-ray studies at a temperature not defined or stated as room temperature. Ehrlich reported the existence of a single phase for the composition BeTi, but did not describe its structure. The only composition to be entirely agreed upon by two observers was that associated with Be_2Ti. Misch and later Ehrlich described this phase as consisting of the three layered Laves cubic phase C_{15} type structure. The lattice parameter agreed by these two observers was a = 6.426A°.

The specimen one prepared for this room temperature analysis

of an equilibrium state obtained at a high temperature consisted of a composition near Be_3Ti_2. This sample was found to be 80 per cent cubic of the three layered Laves C_{15} type structure. The second phase was found to be 18 per cent hexagonal of the two layered Laves C_{14} type structure. The cell of the heat treated cubic phase was found to have a lattice parameter a = 6.460 ± 0.006A. Approximately two per cent of specimen one was pure titanium. Ehrlich had observed a second phase in Be_3Ti_2 also. He associated it with a single BeTi phase, but did not determine its structure. The existence of the hexagonal second phase as the C_{14} type structure as observed here accounts for Ehrlich's observations.

The second specimen examined in this report consisted of a composition on the beryllium rich side of Be_2Ti. This specimen was found to be in the same region of constitution as sample one. The dominant phase was cubic of the three layered Laves C_{15} type structure and comprised 80 per cent of the specimen. An identical cubic parameter was found here as in sample one. More of the hexagonal phase appeared on the beryllium rich side of Be_2Ti than on the titanium rich side. The hexagonal C_{14} type structure had parameters identical to those found in the same phase of specimen one, c = 7.161 ± 0.008A and a = 4.485 ± 0.005A.

Specimen three is identical to specimen two in types of phases, their parameters, and intensities. Zalkin, Sands, Bedford, and Krikorian (10) report the existence of a Be_3Ti phase which is hexagonal as is the minor phase of specimens one, two,

and three. However, they report their Be_3Ti phase as having parameters a = 4.49A and c = 21.32A. This undoubtedly is the same structure as observed in this heat treated phase analysis. Their base parameter is the same as the minor phase's; however, their reported c-parameter is three times that found in this analysis. This is most likely the two layered Laves phase found in the Be_2Ti composition.

The fourth specimen did not reflect the observations of Ehrlich, who explained it as a unique single phase. Specimen four was two phased with the cubic C_{15} type structure remaining as the dominant phase. A new phase comprised 40 per cent of the specimen. This was a phase isomorphous with Nb_2Be_{17}. The parameters of this new phase were found to be a = 7.454A and c = 10.72A°. This phase had been reported by Paine and Carrabine with the parameters a = 7.34A and c = 10.73A. Zalkin, Sands, Bedford, and Krikorian observed this phase on the beryllium poor side of $Be_{17}Ti_2$, and described it as α-$Be_{17}Ti_2$ with parameters a = 7.392A and c = 10.79A°. Within this two phased region, the hexagonal structure reported here is extremely beryllium poor contributing to a crowding within the c-dimension and a bulging of the a-dimension.

Specimen five differed very slightly in composition from sample four. This sample was found to be 55 per cent cubic of the C_{15} type structure and 45 per cent hexagonal which is isomorphous to Nb_2Be_{17}. The cubic and hexagonal structures' parameters agreed with those stated for specimen four.

An analysis of specimens six and seven was hoped to provide

information about the α and β phases reported by Zalkin, Sands, Bedford, and Krikorian, and the $Be_{17}Ti_2$ phase of Paine and Carrabine. Specimens six and seven consisted of compositions very near Be_6Ti. These specimens were found to be 30 per cent cubic of the C_{15} type structure, 60 per cent hexagonal isomorphous to Nb_2Be_{17}, and 10 per cent of the dominant cubic phase of specimen eight. It is unlikely that a single phase near $Be_{17}Ti_2$ could exist if small portions of a $Be_{12}Ti$ phase appear in a Be_6Ti specimen. The β-$Be_{17}Ti_2$ phase reported in literature was hexagonal with parameters a = 7.36A and c = 7.30A. This β phase was reported on the beryllium rich side of $Be_{17}Ti_2$, and therefore its presence in specimen eight was expected.

Specimen eight consisted of a composition near $Be_{12}Ti$. Zalkin, Sand, Bedford, and Krikorian reported that the disordered hexagonal $Be_{12}Ti$ phase detected by Rauechle and Rundle was not observed in their powder patterns. Specimen eight consisted of 90 per cent cubic similar to $CrAl_{12}$ and 10 per cent hexagonal. The cubic lattice parameter was found to be a = 7.38 ± 0.02A°. The placement of the atoms within this phase was not accomplished.

SUMMARY

A literature search has yielded five papers that announce the existence of phases within the system of titanium-beryllium that in several instances are not wholly agreed upon. The purpose of this report is to supply continuity to existing intermetallic phases and to detect and analyze new structures if

disagreement is found. At the present time, all the reports relative to this binary system have either neglected to define the temperature state of investigation or have stated it as room temperature.

In order to obtain a room temperature analysis of an equilibrium established at a high temperature, eight specimens were heat treated to 1026 ± 25° C for a period of 67 hours 20 minutes and then quenched rapidly to 33° C. The specimens were then analyzed metallographically and by the x-ray powder diffraction technique. Chemical and density considerations were applied, yielding additional information about the phases within the eight samples.

Four distinct phases were observed within the range of composition studied. A cubic phase of the three layered Laves C_{15} type structure was observed in specimens one through seven. This was the dominant phase in specimens one, two, and three. Within these three specimens a constant lattice parameter was found to be a = 6.460 ± 0.006A°. A constant parameter is expected in these three specimens since they were all multiphased. This value agrees well with Ehrlich's value a = 6.456A° observed in Be_3Ti. The two layered Laves C_{14} type structure previously unreported was observed in specimens one, two, and three. This phase had not been found in this binary system even though the conditions that apply to the C_{15} type structure also apply to the C_{14} type. The lattice parameters of this phase were found to be constant with a = 4.485A° and c = 7.161A°. This should be compared with the parameters a = 4.49A° and c = 21.32/3 A° found

to apply to a hexagonal structure of Be_3Ti in the literature. A great possibility exists that the published c-dimension does not apply to the basic unit cell. Specimens four through seven were on the beryllium poor side of $Be_{17}Ti_2$ and contained the α-$Be_{17}Ti_2$ phase reported in literature. This phase had constant parameters of a = 7.454A° and c = 10.72A°. The c-dimension agrees with the published values but the a-dimension is 0.06A° larger than the nearest published value. This may be due to the fact that all four specimens containing this phase were very beryllium poor with respect to a true $Be_{17}Ti_2$ composition. The two published values for the a-dimension also differ by more than the 0.05A°. Small amounts of the previously reported β-$Be_{17}Ti_2$ phase were observed in specimen eight. This specimen consisted of a dominant cubic phase with a parameter a = 7.38 $\pm$ 0.02A°. This phase is believed to be similar to $CrAl_{12}$.

FUTURE STUDY

The information provided in this report analyzes the regions of composition between pure titanium and $Be_{12}Ti$. Since evidence of pure Ti was found in Be_3Ti_2, the possibility of a unique phase between Ti and Be_3Ti_2 is quite remote. In order to assure this prediction a specimen of $BeTi_2$ should be examined. The evidence of β-$Be_{17}Ti_2$ in the $Be_{12}Ti$ specimen discounts the possibility of a new phase occurring on the beryllium poor side of $Be_{12}Ti$. However, an investigation of specimens of compositions on the beryllium rich side of $Be_{12}Ti$, such as $Be_{14}Ti$, $Be_{18}Ti$, and $Be_{24}Ti$

Table 3. Published and present results of structural data for the titanium-beryllium system.

Structure type	Structure	Parameters	Density	Molecular units / Unit cell	Authors
Nb_2Be_{17}	Hex	a = 7.34A c = 10.73A	2.476	3	Paine & Carrabine
Nb_2Be_{17}	Hex, defined as α-$Be_{17}Ti_2$	a = 7.392 c = 10.79	2.428	3	Zalkin, Sands, Bedford, Krikorian
Nb_2Be_{17}	Hex	a = 7.454 c = 10.72	2.577	3	Present work
$MgCu_2$	Cubic as seen in Be_3Ti	a = 6.456	3.285	8	Ehrlich
$MgCu_2$	Cubic as seen in Be_2Ti	a = 6.427	3.297	8	Misch
$MgCu_2$	Cubic	a = 6.460	3.242	8	Present work
Compound Be_3Ti	Hex	a = 4.49 c = 21.32			Zalkin, Sands, Bedford, Krikorian
Structure Type $MgZn_2$	Hex	a = 4.485 c = 7.161	3.509	4	Present work
Specimen eight	Cubic	a = 7.38	2.62	4	Present work
Th_2Ni_{17}	Hex, defined as β-$Be_{17}Ti_2$	a = 7.36 c = 7.30	2.41	4	Zalkin, Sands, Bedford, Krikorian

should provide enough intermetallic phase data to describe in general regions the system of titanium-beryllium.

The heat treatment method, temperature, and time should be applied to future investigations of this system. The phase agreement found between this report and published data at room temperature should discount the necessity of heat treatment investigations at temperature such as 800° C and 600° C. At the beginning of the heat treatment the samples should be taken to 1100° C and gradually reduced to 1026° C. This should minimize the effect of an energy barrier if one exists near 1000°C.

A voltage regulator and an automatic temperature time recording device would remove much of the unnecessary trouble associated with the heat treatment.

ACKNOWLEDGMENT

The author is highly indebted to Dr. R. Dean Dragsdorf for his constant advice and encouragement throughout the study of this problem and the logic behind the adaption of this problem to the IBM-650 data processing machine.

LITERATURE CITED

1. Ehrlich, P.
Das system titan-beryllium. Z. Anorg. Chem. 259:1-2. 1949.

2. Freeman, H. C. and J. D. W. L. Smith.
A polynomial approximation to atomic scattering curves. Acta Cryst. 11:819-822. 1958.

3. Klee, H. and H. Witte.
Magnetische suszeptibilitaten ternarer magnesium legierungen und ihre deutung vom standpunkt der elektronentheorie der metalle. Z. Physik. Chem., 202:352. 1954.

4. Misch, L.
Metallwirtschaft, 15:163. 1936.

5. Paine, R. M. and J. A. Carrabine.
Some new intermetallic compounds of beryllium. Acta Cryst., 13:680-681. 1960.

6. Pauling, L., and others.
The electronic structure of metals and alloys. Cleveland: American Society of Metals, 1956.

7. Rauchle, R. F., and R. E. Rundle.
The structure of $TiBe_{12}$. Acta Cryst., 5:85. 1952.

8. Sax, N. I.
Handbook of dangerous materials. New York: Reinhold Publishing Corporation. 1:46-48. 1951.

9. White, D. W., and J. E. Burke.
The metal beryllium. Cleveland: American Society on Metals, 1955.

10. Zalkin, A., and others.
The beryllides of Ti, V, Cr, Zr, Nb, Mo, Hf, and Ta. Acta Cryst., 14:63-64. 1961.

APPENDIX

Table 4. Observed and calculated $1/d^2$ and intensity values* for α-Be_2Ti, $MgCu_2$ type structure.

hkl	$1/d^2$ (obs)	$1/d^2$ (calc)	Intensity (obs)	Intensity (calc)
111	0.0769	0.07188	S	91
220	0.2010	0.1917	VS	100
311	0.2745	0.2636	VS	81
331	0.4682	0.4554	W	14
422	0.5890	0.5752	S	31
511-333	0.6608	0.6471	S	27
440	0.7810	0.7669	M	20
531	0.8525	0.8388	W	15
620	0.9727	0.9586	M	27
533	1.0415	1.0306	W	22
711-551	1.2333	1.2223	W	56
642	1.3537	1.3419	S	45
731	1.4234	1.4138	S	27
800	1.5365	1.5336	W	13
733	1.6093	1.6055	W	15

Cubic structure a = 6.460 ± 0.006 A

$$\frac{\text{molecular units}}{\text{cell}} = 8$$

8 Ti - 000, $\frac{1}{2}\frac{1}{2}0$, $\frac{1}{2}0\frac{1}{2}$, $0\frac{1}{2}\frac{1}{2}$, 1/4 1/4 1/4, 3/4 3/4 1/4,
3/4 1/4 3/4, 1/4 3/4 3/4.

16 Be - 5/8 5/8 5/8, 1/8 1/8 5/8, 1/8 5/8 1/8, 5/8 1/8 1/8,
7/8 7/8 5/8, 3/8 3/8 5/8, 3/8 7/8 1/8, 7/8 3/8 1/8,
7/8 5/8 7/8, 3/8 1/8 7/8, 3/8 5/8 3/8, 7/8 1/8 3/8,
5/8 7/8 7/8, 1/8 3/8 7/8, 1/8 7/8 3/8, 5/8 3/8 3/8.

*Observed intensities taken from specimen two's photograph which is 80% α-Be_2Ti, 20% β-Be_2Ti.

Table 5. Observed and calculated $1/d^2$ and intensity values* for β-Be_2Ti, $MgZn_2$ type structure.

hkl	$1/d^2$ (obs)	$1/d^2$ (calc)	Intensity (obs)	Intensity (calc)
100		0.0663		74
002	0.0740	0.0780	S*	118 44
011		0.0858		38
012	0.1444	0.1443	VW	36
110	0.1972	0.1989	VS*	88
013	0.2402	0.2418	W	100
200	0.2710	0.2652	VS*	72 15
112		0.2769		57
021	0.2850	0.2847	M	20
022		0.3432		3
014	0.3893	0.3783	W	11 6
023		0.4407		2
120	0.4628	0.4641	M*	12 6
121		0.4836		6
122	0.5260	0.5421	VVW	40 4
015		0.5538		36
300	0.5823	0.5967	S*	25
123	0.6354	0.6396	W	29
032	0.6560	0.6747	S*	17
025	0.7752	0.7527	M*	19 15
124		0.7761		4
220	0.7992	0.7956	M	13
130		0.8619		2
222	0.8710	0.8736	VVW	10 6
131		0.8814		2
116	0.9074	0.9009	VVW	5
125	0.9495	0.9516	VVW	12
026	0.9682	0.9672	M*	3
133	1.0393	1.0374	W*	22 19
041		1.0803		3
042	1.1662	1.1388	VVW*	11 6
126		1.1661		5
043	1.2280	1.2363	W*	6
230	1.2591	1.2597	VVW	2
036	1.2849	1.2987	VVW	3
018	1.3305	1.3143	VVW	4
135	1.3486	1.3494	S*	17
140		1.3923		16
127	1.4210	1.4196	S*	36 6
233		1.4352		14
118	1.4660	1.4469	VVW	17
226	1.4927	1.4976	VVW	17 12
028		1.5132		5

*Observed intensities taken from specimen's three photograph which is 70% α-Be Ti, 30% β-Be Ti.

Table 5 (concl.).

Hexagonal structure $a = 4.485 \pm 0.005$ A

$c = 7.161 \pm 0.008$ A

$$\frac{\text{molecular units}}{\text{unit cell}} = 4$$

4 Tl - $\pm(1/3, 2/3, 1/16)$, $\pm(1/3\ 2/3\ 7/16)$

8 Be - 000, $00\frac{1}{8}$, $\pm(1/6, 1/3, 3/4)$, $\pm(1/3, 1/16, 1/4)$,
$\pm(5/6, 1/6, 1/4)$

Table 6. Observed and calculated $1/d^2$ and intensity values* for α-$Be_{17}Ti_2$, Nb_2Be_{17} type structure.

hkl	$1/d^2$ (obs)	$1/d^2$ (calc)	Intensity (obs)	Intensity (calc)
110	0.0771	0.0720	S	98 74
003		0.0783		24
021	0.0857	0.1047	VW	29
113	0.1591	0.1503	VS	100
121	0.1818	0.1767	M	32
122	0.2050	0.2028	M	21
300	0.2166	0.2160	M	53
024	0.2417	0.2352	W	43 33
015		0.2415		10
220	0.2734	0.2880	M	43
033	0.2883	0.2943	S	84
124	0.3044	0.3072	VS	57 37
006		0.3132		20
131	0.3246	0.3207	VW	12
132	0.3359	0.3468	VW	8
134	0.4469	0.4512	VW	19
231	0.4752	0.4647	VW	6
140	0.5062	0.5040	M	7
027		0.5223		7
036	0.5460	0.5292	M	21 14
143	0.5843	0.5823	M	18
127		0.5943		42 13
234		0.5952		11
226	0.6158	0.6012	M	17
330	0.6501	0.6480	VW	8
333	0.7293	0.7263	W	19
137	0.7467	0.7383	W	9
119	0.7736	0.7767	VW	7
244	0.8059	0.8112	W	8
600	0.8648	0.8640	VW	16
237		0.8823		13 7
154	0.8887	0.8832	VW	6
039	0.9299	0.9207	VW	6
336	0.9505	0.9612	VW	17
253	1.0131	1.0143	W	9
440	1.1439	1.1520	VW	7
157		1.1703		7
164	1.1794	1.1712	M	33 6
066		1.1772		20
149	1.2294	1.2087	VW	11
347		1.3143		14 7
354	1.2966	1.3152	W	7
339	1.3670	1.3527	W	17
624	1.3923	1.3872	VW	9

Table 6 (concl.).

hkl	$1/d^2$ (obs)	$1/d^2$ (calc)	Intensity (obs)	Intensity (calc)
173	1.4380	1.4463	W	14
167		1.4583		10
446	1.4664	1.4652	S	13
03·12		1.4688	52	10
360		1.5120		19
22·12		1.5408		16
24·10		1.5420		10
069	1.5739	1.5687	120	8
02·13		1.5693	S	7
633		1.5903		79
357	1.6129	1.6023	VW	18
21·13	1.6496	1.6383	S	25

Hexagonal structure $a = 7.454 \pm 0.008$ A
$c = 10.72 \pm 0.07$ A

$\frac{\text{molecular units}}{\text{cell}} = 3$

6 Ti - $\pm(0, 0, z)$ + (0, 0, 0; 1/3, 2/3, 2/3; 2/3, 1/3, 1/3), $z = 0.16$

6 Be_I - $\pm(0, 0, z')$ + (0, 0, 0; 1/3, 2/3, 2/3; 2/3, 1/3, 1/3), $z' = 0.40$

9 Be_{II} - $(\frac{1}{2}, 0, 0; 0, \frac{1}{2}, 0; \frac{1}{2}, \frac{1}{2}, 0)$ + (0, 0, 0; 1/3, 2/3, 2/3; 2/3, 1/3, 1/3)

18 Be_{III} - $\pm(x, 0, \frac{1}{2}; 0, x, \frac{1}{2}; x, x, \frac{1}{2})$ + (0, 0, 0; 1/3, 2/3, 2/3; 2/3, 1/3, 1/3), $x = 0.33$

18 Be_{IV} - $\pm(x', \bar{x}', z'; x', 2x', z'; 2\bar{x}', \bar{x}', z')$ + (0, 0, 0; 1/3, 2/3, 2/3, 2/3, 1/3, 1/3), $z' = 0.01$, $x' = 0.167$

*Observed intensities taken from specimen six's photograph which is 30% C_{15} type structure, 60% Nb_2Be_{17}, and 10% $Be_{12}Ti$.

Table 7. Observed and calculated $1/d^2$ and intensity values* for specimen one.

Identity	hkl	$1/d^2$ (obs)	$1/d^2$ (calc)	Intensity (obs)	Intensity (calc)
Hex	100		0.0663		74
Cubic	111		0.0719		91
Hex	002	0.0755	0.0780	S	44
Hex	011		0.0858		38
Hex	012	0.1460	0.1443	VW	36
TiSi		0.1729		VVW	
Cubic	220		0.1917		100
Hex	110	0.1990	0.1989	VS	88
Hex	013	0.2423	0.2418	VW	100
Cubic	311		0.2636		81
Hex	200		0.2652		15
Hex	112	0.2738	0.2769	VS	57
Hex	021		0.2847		20
Hex	122		0.3432		3
Hex	014	0.3912	0.3783	W	6
Hex	023		0.4407		2
Cubic	331		0.4554		14
Hex	120	0.4659	0.4641	M	6
Hex	121		0.4836		6
Hex	122	0.5227	0.5421	VVW	4
Hex	015		0.5538		36
Cubic	422	0.5857	0.5752	S	31
Hex	300		0.5967		25
Hex	123	0.6371	0.6396	VW	29
Cubic	511-333		0.6471		27
Hex	032	0.6601	0.6747	S	17
Hex	025		0.7527		15
Cubic	440		0.7669		20
Hex	124	0.7757	0.7761	M	4
Hex	220		0.7956		13
Cubic	531	0.8487	0.8388	M	15
Hex	130		0.8619		2
Hex	222		0.8736		6
Hex	131		0.8814		2
Hex	116	0.9285	0.9009	VVW	5
Hex	125		0.9516		12
Cubic	620	0.9578	0.9586	VVW	27
Hex	026	0.9699	0.9672	S	3
Cubic	533		1.0306		22
Hex	133	1.0410	1.0393	M	19
Hex	041		1.0803		3
Hex	042		1.1388		6
Hex	126	1.1602	1.661	VW	5
Cubic	711-551	1.1921	1.2223	VW	56

Table 7 (concl.).

Identity	hkl	$1/d^2$ (obs)	$1/d^2$ (calc)	Intensity (obs)	Intensity (calc)
Hex	043	1.2307	1.2363	M	6
Hex	230	1.2591	1.2597	VVW	2
Hex	036	1.2899	1.2987	VVW	3
Hex	018		1.3143		4
Cubic	642	1.3300	1.3419	VVW	45
Hex	135	1.3518	1.3494	VS	17
Hex	140		1.3923		16
Cubic	731		1.4138		27
Hex	127	1.4213	1.4196	VS	6
Hex	233		1.4352		14
Hex	118		1.4469		17
Hex	226	1.4919	1.4976	VVW	12
Hex	028		1.5132		5
Cubic	800	1.5370	1.5336	VW	13
Cubic	733	1.6088	1.6055	W	15

*The calculated intensity values are taken from pure phase calculations.

Table 8. Observed and calculated $1/d^2$ and intensity values* for specimen two.

Identity	hkl	$1/d^2$ (obs)	$1/d^2$ (calc)	Intensity (obs)	Intensity (Calc)
Hex	100		0.0663		74
Cubic	111		0.0719		91
Hex	002	0.0740	0.0780	S	44
Hex	011		0.0858		38
Hex	012	0.1444	0.1443	VW	36
TiSi		0.1820		W	
Cubic	220		0.1917		100
Hex	110	0.1972	0.1989	VS	88
TiSi		0.2149		VW	
Hex	013	0.2402	0.2418	W	100
Cubic	311		0.2636		81
Hex	200	0.2710	0.2652	VS	15
Hex	112		0.2769		57
Hex	021	0.2850	0.2847	M	20
Hex	122		0.3432		3
Hex	014	0.3893	0.3783	W	6
Hex	023		0.4407		2
Cubic	331		0.4554		14
Hex	120	0.4628	0.4641	M	6
Hex	121		0.4836		6
Hex	122	0.5260	0.5421	VVW	4
Hex	015		0.5538		36
Cubic	422		0.5752		31
Hex	300	0.5823	0.5967	S	25
Hex	123	0.6354	0.6396	W	29
Cubic	511-333		0.6471		27
Hex	032	0.6560	0.6747	S	17
Hex	025		0.7527		15
Cubic	440		0.7669		20
Hex	124	0.7752	0.7761	M	4
Hex	220	0.7992	0.7956	M	13
Cubic	531		0.8388		15
Hex	130		0.8619		2
Hex	222	0.8710	0.8736	VVW	6
Hex	131		0.8814		2
Hex	116	0.9074	0.9009	VVW	5
Hex	125	0.9495	0.9516	VVW	12
Cubic	620		0.9586		27
Hex	026	0.9682	0.9672	M	3
Cubic	533		1.0306		22
Hex	133	1.0393	1.0374	W	19
Hex	041		1.0803		3
Hex	042		1.1388		6
Hex	126	1.1662	1.1661	VVW	5
Cubic	711-551		1.2223		56

Table 8 (concl.).

Identity	hkl	$1/d^2$ (obs)	$1/d^2$ (calc)	Intensity (obs)	Intensity (calc)
Hex	043	1.2280	1.2363	W	6
Hex	230	1.2591	1.2597	VVW	2
Hex	036	1.2849	1.2987	VVW	3
Hex	018	1.3305	1.3143	VVW	4
Cubic	642		1.3419		45
Hex	135	1.3486	1.3494	S	17
Hex	140		1.3923		16
Cubic	731		1.4138		27
Hex	127	1.4210	1.4196	S	6
Hex	233		1.4352		14
Hex	118	1.4660	1.4469	VVW	17
Hex	226	1.4927	1.4976	VVW	12
Hex	028		1.5132		5
Cubic	800	1.5368	1.5336	W	13
Cubic	733	1.6088	1.6055	VW	15

*The calculated intensity values are taken from pure phase calculations.

Table 9. Observed and calculated $1/d^2$ and intensity values* for specimen three.

Identity	hkl	$1/d^2$ (obs)	$1/d^2$ (calc)	Intensity (obs)	Intensity (calc)
Hex	100		0.0663		74
Cubic	111	0.0731	0.0719	M	91
Hex	002		0.0780		44
Hex	011		0.0858		38
Hex	012		0.1443		36
TiSi		0.1761		M	
Cubic	220		0.1917		100
Hex	110	0.1987	0.1989	VS	88
Hex	013		0.2418		100
Cubic	311		0.2636		81
Hex	200	0.2676	0.2652	VS	15
Hex	112		0.2769		57
Hex	021	0.2832	0.2847	M	20
Hex	122	0.3324	0.3432	VVW	3
Hex	014	0.3764	0.3783	VVW	6
Hex	023	0.4097	0.4407		2
Cubic	331	0.4617	0.4554	VVW	14
Hex	120		0.4641	W	6
Hex	121	0.5011	0.4836	VW	6
Hex	122		0.5421		4
Hex	015		0.5538		36
Cubic	422	0.5801	0.5752	S	31
Hex	300	0.6105	0.5967	VW	25
Hex	123		0.6396		29
Cubic	551-333	0.6515	0.6471	M	27
Hex	032	0.6747	0.6747	VW	17
Hex	025		0.7527		15
Cubic	440		0.7669		20
Hex	124	0.7729	0.7761	M	4
Hex	220	0.7958	0.7956	VW	13
Cubic	531	0.8478	0.8388	W	15
Hex	130	0.8699	0.8619	VVW	2
Hex	222		0.8736		6
Hex	131		0.8814		2
Hex	116	0.8963	0.9009	VW	5
Hex	125		0.9516		12
Cubic	620		0.9587		27
Hex	026	0.9654	0.9672	M	3
Cubic	533	0.9984	1.0306	VW	22
Hex	133	1.0363	1.0374	W	19
Hex	041	1.0948	1.0803	VVW	3
Hex	042		1.1388		6
Hex	126	1.1667	1.1661	VVW	5

Table 9 (concl.).

Identity	hkl	$1/d^2$ (obs)	$1/d^2$ (calc)	Intensity (obs)	Intensity (calc)
Cubic	711-551	1.2280	1.2223	W	56
Hex	043		1.2363		6
Hex	230	1.2605	1.2597	VVW	2
Hex	036	1.2907	1.2987	W	3
Hex	018		1.3143		4
Cubic	642	1.3471	1.3419	S	45
Hex	135		1.3494		17
Hex	140	1.3877	1.3923	VW	16
Cubic	731		1.4138		27
Hex	127	1.4196	1.4196	S	6
Hex	233		1.4352		14
Hex	118	1.4660	1.4469	W	17
Hex	226	1.4828	1.4976	VVW	12
Hex	028		1.5132		5
Cubic	800	1.5340	1.5336	VVW	13
Cubic	733	1.6080	1.6055	VW	15

*The calculated intensity values are taken from pure phase calculations.

Table 10. Observed and calculated $1/d^2$ and intensity values* for specimen four.

Identity	hkl	$1/d^2$ (obs)	$1/d^2$ (calc)	Intensity (obs)	Intensity (calc)
Cubic	111	0.0738	0.0719	M	91
Hex	110		0.0720		74
Hex	003	0.0848	0.0783	VW	24
Hex	021		0.1047		29
Hex	113	0.1589	0.1503	S	100
Hex	121		0.1767		32
Cubic	220	0.1820	0.1917	S	100
Hex	122	0.2048	0.2028	S	21
Hex	300		0.2160		53
Hex	024	0.2238	0.2352	VW	33
Hex	015	0.2425	0.2415	VW	10
Cubic	311	0.2567	0.2636	VW	81
Hex	220	0.2745	0.2880	M	43
Hex	033	0.2885	0.2943	S	84
Hex	124	0.3051	0.3072	VS	37
Hex	006		0.3132		20
Hex	131	0.3346	0.3207	VW	12
Hex	132	0.3806	0.3468	VW	8
Hex	134	0.4118	0.4512	VW	19
Cubic	331		0.4554		14
Hex	231	0.4752	0.4647	VW	6
Hex	140	0.5089	0.5040	W	7
Hex	027		0.5223		7
Hex	036	0.5452	0.5292	VW	14
Cubic	422		0.5752		31
Hex	143	0.5834	0.5823	M	18
Hex	127		0.5943		13
Hex	234		0.5952		11
Hex	226	0.6166	0.6012	W	17
Cubic	511-333	0.6615	0.6471	VVW	27
Hex	330	0.6831	0.6480	VW	8
Hex	333	0.7066	0.7263	W	19
Hex	137	0.7310	0.7383	VVW	9
Cubic	440		0.7669		20
Hex	119	0.7749	0.7767	VVW	7
Hex	244	0.8040	0.8112	W	8
Cubic	531		0.8388		15
Hex	600	0.8637	0.8640	VW	16
Hex	237		0.8823		7
Hex	154		0.8832		6
Hex	039	0.9007	0.9207	VW	6
Cubic	620	0.9495	0.9586	VVW	27
Hex	336	0.9703	0.9612	W	17
Hex	253	1.0064	1.0143	VW	9
Cubic	533	1.0309	1.0306	VVW	22
Hex	440	1.0644	1.1520	VW	7

Table 10 (concl.).

Identity	hkl	$1/d^2$ (obs)	$1/d^2$ (calc)	Intensity (obs)	Intensity (calc)
Hex	157	1.0912	1.1703	VW	7
Hex	164	1.1305	1.1712	VVW	6
Hex	066	1.1730	1.1772	W	20
Hex	149	1.2283	1.2087	VVW	11
Cubic	711-551	1.2887	1.2223	W	56
Hex	347		1.3143		7
Hex	354	1.3181	1.3152	VVW	7
Cubic	642		1.3419		45
Hex	339	1.3606	1.3527	VVW	17
Hex	624	1.3837	1.3872	W	9
Cubic	731	1.4281	1.4138	VVW	27
Hex	173		1.4463		14
Hex	167		1.4583		10
Hex	446	1.4625	1.4652	M	13
Hex	03·12	1.4876	1.4688	VW	10
Hex	360		1.5120		19
Cubic	800	1.5291	1.5336	VW	13
Hex	22·12		1.5408		16
Hex	24·10		1.5420		10
Hex	069	1.5637	1.5687	M	8
Hex	02·13	1.5723	1.5693	M	7
Hex	633		1.5903		79
Hex	357		1.6023		18
Cubic	733	1.6265	1.6055	VW	15
Hex	21·13	1.6466	1.6383	W	25

*The calculated intensity values are taken from pure phase calculations.

Table 11. Observed and calculated $1/d^2$ and intensity values* for specimen five.

Identity	hkl	$1/d^2$ (obs)	$1/d^2$ (calc)	Intensity (obs)	Intensity (calc)
Cubic	111		0.0719		91
Hex	110	0.0750	0.0720	M	74
Hex	003	0.0845	0.0783	S	24
Hex	021	0.0970	0.1047	VVW	29
Hex	113	0.1592	0.1503	M	100
Hex	121		0.1767		32
Cubic	220	0.1816	0.1917	VS	100
Hex	122	0.2060	0.2028	S	21
Hex	300	0.2176	0.2160	M	53
Hex	024		0.2352		33
Hex	015	0.2452	0.2415	VW	10
Cubic	311	0.2565	0.2636	VW	81
Hex	220	0.2741	0.2880	S	43
Hex	033	0.2877	0.2943	S	84
Hex	124	0.3047	0.3072	S	37
Hex	006		0.3132		20
Hex	131	0.3309	0.3207	VVW	12
Hex	132	0.3808	0.3468	VW	8
Hex	134	0.4142	0.4512	VW	19
Cubic	331	0.4502	0.4554	VW	14
Hex	231	0.4770	0.4647	W	6
Hex	140	0.5086	0.5040	M	7
Hex	027		0.5223		7
Hex	036		0.5292		14
Cubic	422	0.5507	0.5752	VW	31
Hex	143	0.5868	0.5823	M	18
Hex	127		0.5943		13
Hex	234		0.5952		11
Hex	226	0.6161	0.6012	W	17
Cubic	511-333	0.6468	0.6471	VW	27
Hex	330	0.6647	0.6480	VVW	8
Hex	333	0.6865	0.7263	VW	19
Hex	137	0.7057	0.7383	M	9
Cubic	440	0.7343	0.7669	VW	20
Hex	119	0.7829	0.7767	VW	7
Hex	244	0.8039	0.8112	M	8
Cubic	531		0.8388		15
Hex	600		0.8640		16
Hex	237		0.8823		7
Hex	154		0.8832		6
Hex	039	0.9069	0.9207	W	6
Cubic	620	0.9443	0.9586	VVW	27
Hex	336	0.9793	0.9612	W	17
Hex	253	1.0133	1.0143	VW	9

Table 11 (concl.).

Identity	hkl	$1/d^2$ (obs)	$1/d^2$ (calc)	Intensity (obs)	Intensity (calc)
Cubic	533	1.0427	1.0306	VVW	22
Hex	440	1.0694	1.1520	VVW	7
Hex	157	1.0981	1.1703	VW	7
Hex	164	1.1419	1.1712	VVW	6
Hex	066	1.1807	1.1772	M	20
Hex	149	1.2044	1.2087	VVW	11
Cubic	711-551	1.2337	1.2223	VVW	56
Hex	347	1.2662	1.3143	VVW	7
Hex	354	1.2984	1.3152	M	7
Cubic	642	1.3396	1.3419	VVW	45
Hex	339	1.3514	1.3527	VVW	17
Hex	624	1.3718	1.3872	VW	9
Cubic	731	1.3942	1.4138	W	27
Hex	173	1.4367	1.4463	VW	14
Hex	167		1.4583		10
Hex	446		1.4652		13
Hex	03·12	1.4724	1.4688	M	10
Hex	360	1.4995	1.5120	VW	19
Cubic	800	1.5336	1.5336	VW	13
Hex	22·12		1.5408		16
Hex	24·10		1.5420		10
Hex	069	1.5684	1.5687	M	8
Hex	02·13	1.5771	1.5693	M	7
Hex	633		1.5903		79
Hex	357	1.6064	1.6023	VW	18
Cubic	733		1.6055		15
Hex	21·13	1.6302	1.6383	VW	25

*The calculated intensity values are taken from pure phase calculations.

Table 12. Observed and calculated** $1/d^2$ and intensity values for specimen six.

Identity	hkl	$1/d^2$ (obs)	$1/d^2$ (calc)	Intensity (obs)	Intensity (calc)
Cubic	111	0.0639	0.0719	VW	91
Hex	110		0.0720		74
Cubic*	200	0.0771	0.0774	S	
Hex	003	0.0857	0.0783	VW	24
Hex	021	0.0955	0.1047	VVW	29
Hex	113	0.1134	0.1503	VVW	100
Cubic*	220	0.1429	0.1541	VVW	
Hex	121	0.1591	0.1767	VW	32
Cubic	220	0.1695	0.1917	VVW	100
Hex	122	0.1818	0.2028	M	21
Hex	300	0.2050	0.2160	M	53
Cubic*	222	0.2166	0.2279	M	
Hex	024	0.2253	0.2352	M	33
Hex	015	0.2417	0.2415	W	10
Cubic	311	0.2525	0.2636	W	81
Hex	220	0.2734	0.2880	M	43
Hex	033	0.2883	0.2943	S	84
Cubic*	400	0.3044	0.3041	VS	
Hex	124		0.3072		37
Hex	006		0.3132		20
Hex	131	0.3246	0.3207	VW	12
Hex	132	0.3359	0.3268	VW	8
Cubic*	420		0.3795		
Hex	134	0.4469	0.4512	VW	19
Cubic	331		0.4554		14
Hex	231	0.4752	0.4647	VW	6
Hex	140	0.5062	0.5040	M	7
Hex	027		0.5223		7
Hex	036	0.5460	0.5292	M	14
Cubic	422	0.5843	0.5752	M	31
Hex	143		0.5823		18
Hex	127		0.5943		13
Hex	234		0.5952		11
Hex	226		0.6012		17
Cubic*	440	0.6158	0.6033	M	
Cubic	511-333	0.6501	0.6471	VW	27
Hex	330	0.6679	0.6480	VW	8
Hex	330	0.6840	0.7263	VW	19
Hex	137	0.7061	0.7383	W	9
Cubic*	620	0.7293	0.7474	W	
Cubic	442	0.7467	0.7621	W	
Cubic	440	0.7736	0.7669	VW	20
Hex	119		0.7767		7
Hex	244	0.8059	0.8112	W	8
Cubic	531	0.8348	0.8388	VW	15
Hex	600	0.8648	0.8640	VW	16
Hex	237	0.8887	0.8823	VW	7

Table 12 (concl.).

Identity	hkl	$1/d^2$ (obs)	$1/d^2$ (calc)	Intensity (obs)	Intensity (calc)
Hex	154	0.9065	0.8832	W	6
Cubic*	444	0.9299	0.9118	VW	
Hex	039		0.9207		6
Cubic	620	0.9505	0.9586	VW	27
Hex	336	0.9748	0.9612	M	17
Hex	253	1.0131	1.0143	W	9
Cubic	533	1.0395	1.0306	VW	22
Hex	440	1.0674	1.1520	VW	7
Hex	157	1.0985	1.1703	VVW	7
Hex	164	1.1439	1.1712	VW	6
Hex	066	1.1794	1.1772	M	20
Cubic*	800		1.1964		
Hex	149		1.2087	VW	11
Cubic	711-551	1.2294	1.2223	W	56
Hex	347	1.2966	1.3143	W	7
Hex	354		1.3152		7
Cubic	642		1.3419		45
Cubic*	822		1.3483		
Hex	339	1.3670	1.3527	W	17
Hex	624	1.3923	1.3872	VW	9
Cubic	731		1.4138		27
Hex	173	1.4380	1.4463	W	14
Hex	167		1.4583		10
Hex	446		1.4562		13
Hex	03·12	1.4664	1.4688	S	10
Cubic*	840		1.4841		
Hex	360		1.5120		19
Cubic	800		1.5336		13
Hex	22·12		1.5408		16
Hex	24·10		1.5420		10
Hex	069		1.5687		8
Hex	02·13	1.5739	1.5693	S	7
Hex	633		1.5903		79
Hex	357		1.6023		18
Cubic	733	1.6129	1.6055	VW	15
Hex	21·13	1.6496	1.6383	S	25

*Specimen eight cubic.

**The calculated intensity values are taken from pure phase calculations.

Table 13. Observed and calculated** $1/d^2$ and intensity values for specimen seven.

Identity	hkl	$1/d^2$ (obs)	$1/d^2$ (calc)	Intensity (obs)	Intensity (calc)
Cubic	111		0.0719		91
Hex	110		0.0720		74
Cubic*	200	0.0766	0.0774	M	
Hex	003	0.0867	0.0783	W	24
Hex	021		0.1047		29
Hex	113		0.1503		100
Cubic*	220	0.1601	0.1541	VS	
Hex	121	0.1720	0.1767	VVW	32
Cubic	220	0.1833	0.1917	S	100
Hex	122	0.2054	0.2028	W	21
Hex	300	0.2194	0.2160	M	53
Cubic*	222	0.2286	0.2279	M	
Hex	024		0.2352		33
Hex	015	0.2462	0.2415	VW	10
Cubic	311	0.2571	0.2636	VW	81
Hex	220	0.2767	0.2880	M	43
Hex	033	0.2887	0.2943	M	84
Cubic*	400	0.3049	0.3041	VS	
Hex	124		0.3072		37
Hex	006		0.3132		20
Hex	131	0.3219	0.3207	VW	12
Hex	132	0.3335	0.3468	VW	8
Cubic*	420	0.3840	0.3795	VVW	
Hex	134	0.3911	0.4512	VVW	19
Cubic	331	0.4019	0.4554	VVW	14
Hex	231	0.4532	0.4647	VVW	6
Hex	140	0.4741	0.5040	VW	7
Hex	027	0.5073	0.5223	W	7
Hex	036	0.5438	0.5292	W	14
Cubic	422		0.5752		31
Hex	143	0.5860	0.5823	M	18
Hex	127		0.5943		13
Hex	234		0.5952		11
Hex	226	0.6023	0.6012	VW	17
Cubic*	440	0.6170	0.6033	M	
Cubic	511-333	0.6483	0.6471	VVW	27
Hex	330	0.6644	0.6480	VVW	8
Hex	333	0.6840	0.7263	VVW	19
Hex	137	0.7056	0.7383	VW	9
Cubic*	620	0.7305	0.7474	VW	
Cubic*	442	0.7456	0.7621	VW	
Cubic	440		0.7669		20
Hex	119	0.7762	0.7767	W	7
Hex	244	0.8029	0.8112	W	8
Cubic	531	0.8325	0.8388	VW	15
Hex	600	0.8633	0.8640	VVW	16
Hex	237	0.8825	0.8823	VVW	7

Table 13 (concl.).

Identity	hkl	$1/d^2$ (obs)	$1/d^2$ (calc)	Intensity (obs)	Intensity (calc)
Hex	154		0.8832		6
Cubic*	444	0.9024	0.9118	VW	
Hex	039	0.9270	0.9207	W	6
Cubic	620	0.9486	0.9586	W	27
Hex	336	0.9748	0.9612	M	17
Hex	253	1.0097	1.0143	W	9
Cubic	533	1.0378	1.0306	W	22
Hex	440	1.0606	1.1520	VVW	7
Hex	157	1.0950	1.1703	VVW	7
Hex	164	1.1402	1.1712	VVW	6
Hex	066	1.1799	1.1772	M	20
Cubic*	800		1.1964		
Hex	149	1.2166	1.2087	VVW	11
Cubic	711-551	1.2307	1.2223	VW	56
Hex	347	1.2939	1.3143	M	7
Hex	354		1.3152		7
Cubic	642	1.3473	1.3419	W	45
Cubic*	822		1.3483		
Hex	339	1.3663	1.3527	W	17
Hex	624	1.3906	1.3872	VW	9
Cubic	731	1.4212	1.4138	VVW	27
Hex	173	1.4328	1.4463	VVW	14
Hex	167		1.4583		10
Hex	446		1.4562		13
Hex	03·12	1.4635	1.4688	S	10
Cubic*	840	1.4933	1.4841	VVW	
Hex	360	1.5332	1.5120	W	19
Cubic	800		1.5336		13
Hex	22·12		1.5408		16
Hex	24·10		1.5420		10
Hex	069	1.5664	1.5687	S	8
Hex	02·13	1.5746	1.5693	S	7
Hex	633		1.5903		79
Hex	357	1.6120	1.6023	M	18
Cubic	733	1.6483	1.6055	S	15
Hex	21·13	1.6563	1.6383	W	25

*Specimen eight cubic.

**The calculated intensity values are taken from pure phase calculations.

Table 14. Observed $1/d^2$ and intensities for specimen eight.

Identity	hkl	$1/d^2$ (obs)	Intensity (obs)
Hex		0.0459	VW
Cubic	200	0.0774	M
Hex		0.0947	VW
Hex		0.1216	VW
Cubic	220	0.1541	S
Hex		0.1969	VW
Cubic	222	0.2279	S
Hex		0.2470	VVW
Hex		0.2731	VVW
Cubic	400	0.3041	VS
Hex		0.3409	VVW
Cubic	420	0.3795	VVW
Hex		0.4124	VVW
Hex		0.4932	VVW
Hex		0.5292	W
Cubic	440	0.6033	M
Hex		0.6447	VVW
Hex		0.6726	VVW
Cubic	620	0.7474	VW
Cubic	442	0.7621	VVW
Hex		0.7952	VVW
Hex		0.8224	VVW
Hex		0.8557	VVW
Hex		0.8953	W
Cubic	444	0.9118	VW
Hex		0.9731	VW
Hex		1.0296	W
Cubic	800	1.1964	M
Cubic	822	1.3483	W
Cubic	840	1.4841	M
Hex		1.6267	M
Hex		1.6467	M

THE INTERMETALLIC PHASES OF TITANIUM-BERYLLIUM

by

JOHN EDWARD LAWRENCE

B. A., Occidental College, 1959

AN ABSTRACT OF
A MASTER'S THESIS

submitted in partial fulfillment of the

requirements for the degree

MASTER OF SCIENCE

Department of Physics

KANSAS STATE UNIVERSITY
Manhattan, Kansas

1961

The intermetallic phases of eight beryllium rich compositions of the titanium-beryllium system were determined from chemical, metallographical, and x-ray diffraction data. Eight specimens were heat treated at 1026 ± 25°C for 67 hours 20 minutes and then quenched to room temperature for examination. Compositions between Be_3Ti_2 and Be_3Ti contained two major phases. A dominant cubic phase was of the three layered Laves C_{15} type structure with a parameter a = 6.460 ± 0.006A°. The second major phase in this region of composition was hexagonal of the two layered Laves C_{14} type structure with parameters a = 4.485A° and c = 7.161A°. Specimens of composition between Be_4Ti and Be_6Ti were also multiphased with the C_{15} type structure continuing. The α-$Be_{17}Ti_2$ phase reported in literature was found in this region. This phase is isomorphous to Nb_2Be_{17} and has parameters a = 7.454A° and c = 10.72A°. Small amounts of the β-$Be_{17}Ti_2$ phase reported in literature was observed in a specimen of composition near $Be_{12}Ti$. This specimen was primarily a cubic phase with a unit cell parameter a = 7.38 ± 0.02A°.

The intermetallic phases of eight beryllium rich compositions of the titanium-beryllium system were determined from chemical, metallographical, and x-ray diffraction data. Eight specimens were heat treated at 1026 ± 25°C for 67 hours 20 minutes and then quenched to room temperature for examination. Compositions between Be_3Ti_2 and Be_3Ti contained two major phases. A dominant cubic phase was of the three layered Laves C_{15} type structure with a parameter a = 6.460 ± 0.006A°. The second major phase in this region of composition was hexagonal of the two layered Laves C_{14} type structure with parameters a = 4.485A° and c = 7.161A°. Specimens of composition between Be_4Ti and Be_6Ti were also multiphased with the C_{15} type structure continuing. The α-$Be_{17}Ti_2$ phase reported in literature was found in this region. This phase is isomorphous to Nb_2Be_{17} and has parameters a = 7.454A° and c = 10.72A°. Small amounts of the β-$Be_{17}Ti_2$ phase reported in literature was observed in a specimen of composition near $Be_{12}Ti$. This specimen was primarily a cubic phase with a unit cell parameter a = 7.38 ± 0.02A°.